IEEE Access
Multidisciplinary ⋮ Rapid Review ⋮ Open Access Journal

Received 24 June 2022, accepted 7 July 2022, date of publication 15 July 2022, date of current version 21 July 2022.

Digital Object Identifier 10.1109/ACCESS.2022.3191357

RESEARCH ARTICLE

A Novel Network Resolved and Mobile Assisted Cell Search Method for 5G Cellular Communication Systems

JIA-LE YIN[1], MING-CHUN LEE[1], (Member, IEEE), WEI-HAN HSIAO[2], (Member, IEEE), AND CHIA-CHI HUANG[1]

[1]Institute of Communications Engineering, National Yang Ming Chiao Tung University (NYCU), Hsinchu 30010, Taiwan
[2]Department of Electrical Engineering, Chang Gung University (CGU), Taoyuan 33302, Taiwan

Corresponding author: Ming-Chun Lee (mingchunlee@nycu.edu.tw)

This work was supported by the Ministry of Science and Technology (MOST) of Taiwan under Grant MOST 110-2222-E-A49-006, Grant MOST 111-2218-E-A49-024, and Grant MOST 111-2221-E-A49-070.

ABSTRACT When the user equipment (UE) is turned on, it first needs to perform an initial cell search procedure before it can communicate with the base station (BS). However, this procedure must deal with the initial time and frequency synchronization and search for the appropriate home BS for services. In conventional cell search methods, the entire cell search process is carried out on the UE, where the computational requirement can lead to additional overhead and power consumption of the UE. Therefore, aiming to help UEs offloading their overhead to BSs, we in this paper propose a novel cell search method, called *Network Resolved and Mobile Assisted Cell Search*, which can achieve our goal by letting the BSs be the main performers for deciding the appropriate BSs for connection and letting UEs only be the assistants of the cell search process. The implementation details and analysis of the proposed cell search approach are provided along with the numerical simulations. Results show that our proposed cell search not only can offload the computational overhead, but it also outperforms the conventional code-based cell search approach in terms of the cell search error probability with similar overall network energy consumption.

INDEX TERMS Initial cell search, cellular systems, multipath division multiple access (MDMA), universal pilot, base station.

I. INTRODUCTION

When the user equipment (UE) is turned on, it first needs to perform an initial cell search procedure before it can communicate with the base station (BS). This procedure must deal with the initial time and frequency synchronization as well as identify which BS is the most appropriate one to provide service. Only after the initial cell search procedure, the UE can then establish a connection with the corresponding BS. Hence, the initial cell search is critical for the wireless system with BSs.

To conduct the initial cell search, we first need to conduct the time and frequency synchronization. Specifically, the time synchronization includes both symbol time synchronization and frame time synchronization, where the BS and the UE need to work collaboratively on synchronizing their symbol timing and frame timing [1]. Frequency synchronization is to synchronize the carrier frequency between the BS and UE, as the frequency mismatch between them could happen due to the oscillator mismatch, Doppler shift, etc. In general, the frequency mismatch impairments include the fractional carrier frequency offset (FCFO) and integer frequency carrier offset (ICFO) [2]. Therefore, the frequency synchronization mainly includes the estimate and compensate of both the fractional carrier frequency offset and integer carrier frequency offset.

After completing the time and frequency synchronization, the BS and UE then start to collaborate on finding the most appropriate BS for providing the connection. Such BS search and identification process has evolved since the proposition of the first-generation (1G) mobile network system and is

The associate editor coordinating the review of this manuscript and approving it for publication was Nurul I. Sarkar.

continuing its evolution until the announcement of the 5G system [3], and is expected to continue the evolution in the future. Since 1G and 2G are narrowband communication, each BS is assigned a particular control channel (fixed frequency band) to transmit control signals. Based on this control signaling, appropriate BSs for services can be obtained by detecting the power of the control channel [4], [5]. This type of cell search method is known as the *Frequency Based Cell Search*.

Different from the 1G and 2G systems, starting from the 3G system, the mobile communication system has been evolved to be with broadband communications. Therefore, the control channel can no longer be used to identify the BSs. To resolve this issue, in 3G system, each BS is then assigned a particular code so as to enable the UE to distinguish between different BSs by checking what code is received [6]–[11]. Serving as some exemplary references, Refs [6] and [7] discussed the 3rd Generation Partnership Project (3GPP) standard for the initial cell search. The overview of the cell search of the wideband code division multiple access (WCDMA) system was presented in [8] and [9], where the fundamental three steps of the initial cell search were discussed. Also, in [10] and [11], some theoretical analysis and computer simulations of the characteristics of general cell search in the WCDMA system were provided. Although the change of the fundamental multiple access approach from CDMA to orthogonal frequency division multiple access (OFDMA) when 3G system evolved to 4G system has changed the detailed procedure of the initial cell search significantly, the fundamental idea is still using the code to distinguish between the BSs [12]–[17]. Specifically, as pointed out in [12]–[15], the 3GPP standardized initial cell search in LTE and LTE-Advanced systems includes the code into the frequency domain so that the UE can identify the BSs. Although there exist some variant methods for the cell search of 4G system [16], [17], they mostly follow the 3GPP standard, which uses codes to distinguish between the BSs.

Recently, the 5G-NR has been announced, serving as the most popular standard for realizing the 5G system. However, similar to the case of 4G system, the concept of the code-based cell search has again been adopted [18]–[23]. Serving as the exemplary reference, Qualcomm released a white paper on 5G-NR in 2016 [18], where the main focus was on reducing the complexity of cell search via enabling a hierarchical cell search procedure. Later, in 2017, 3GPP announced the first version of the 5G-NR standard [19], [20], specifying both the structure and key properties of NR for the initial cell search, and in [21]–[26], the 3GPP standard for initial cell search in 5G-NR was officially described. Furthermore, in [24]–[26], studies relevant to initial cell search of 5G system were provided. Specifically, in [24], a novel timing synchronization algorithm with anti-frequency offset and anti-noise properties was proposed with the primary synchronization signal (PSS). In [25], a deep-learning-based initial access method for the mmWave MIMO system was proposed. Unlike the conventional methods that use signal energy as the feature for BS detection, the proposed method in [25] used a convolutional neural network model to predict the probability of the existence of PSSs of BSs. Then, based on the predicted probability, it decides whether a BS is detected or not. In [26], a physical-layer cell identity detection method that conducted the 5G-NR initial access by jointly using the frequency offset estimation and the secondary synchronization signal (SSS) sequence was proposed.

To the best of our knowledge, the 5G system also adopts the code-based cell search concept and uses the code embedded in the frequency domain to identify the BSs. Since 3G, 4G, and 5G systems all adopt the code-based concept for cell search, we thus categorize the cell search approaches proposed for them as *Code Based Cell Search* in this paper.

Based on the literature review of the cell search, we observe that conventional code-based cell search methods in 3G, 4G, and 5G systems all require the UE to resolve the corresponding codes of the BSs. Therefore, the entire initial cell search process is performed on the UE, and the BS is only responsible for the regular broadcasting of the control signals to UEs. However, this leads to the computational requirements, and thus the overhead and additional power consumption for UEs. Since there exist situations that require UEs to have very low power and computational consumption [27], [28], we thus in this paper propose a new cell search method whose goal is to help UEs offloading their computational requirements to BSs. Our idea is to let network (BSs) be the main performer of the entire cell search process and the UE is only to assist the network. As a result, large amount of computations can be saved for the UEs. We call this cell search method proposed in this paper the *Network Resolved and Mobile Assisted Cell Search*. We note that in some specific (private) IoT networks for vertical applications, the UEs require very low power and computational consumption [27], [28]. Therefore, the proposed cell search approach that can offload the overhead of UEs to BSs is well-motivated in those networks.

In this paper, the implementation details and the analysis of the proposed network resolved and mobile assisted cell search are presented. Also, simulations are conducted to evaluate the performance of the proposed cell search. Results show that the proposed cell search not only can offload the computational overhead, but it also outperforms the conventional code-based cell search approach in terms of the cell search error probability with similar overall network energy consumption.

The remainder of this paper is organized as follows. Sec. II presents the considered system architecture for the cell search. Sec. III presents the principle of the proposed cell search. In Sec. IV, the detailed procedure of the proposed cell search is provided. Finally, in Sec. V, numerical results that evaluate the proposed cell search approach are provided. We conclude this paper in Sec. VI. Some derivations are relegated to Appendix.

II. MDMA SYSTEM ARCHITECTURE

In order to meet the high data rate and low latency requirements of 5G network, several solutions have been

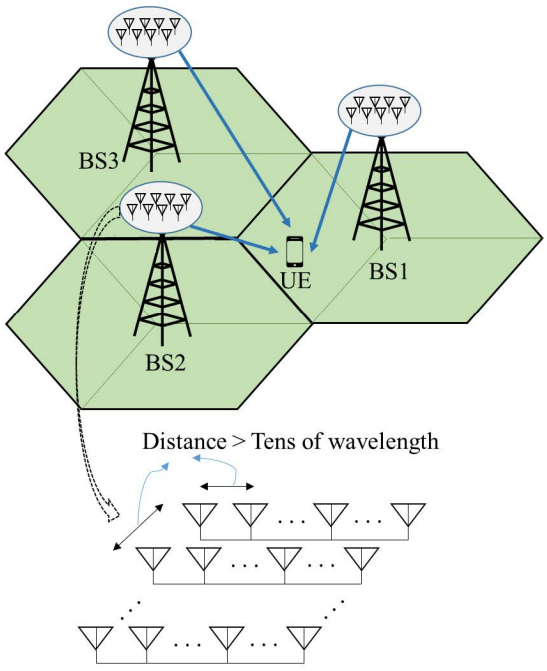

FIGURE 1. The MDMA system cellular layout.

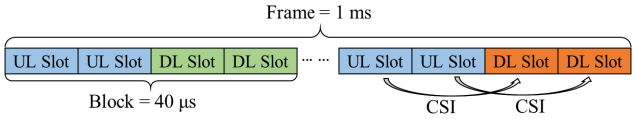

FIGURE 2. Frame structure of the considered MDMA system.

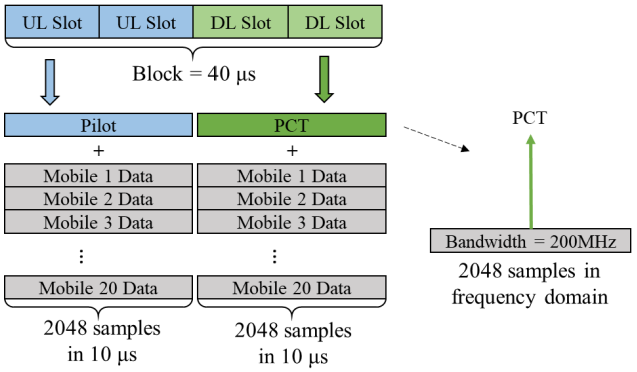

FIGURE 3. Symbol structure.

proposed [29], such as heterogeneous networks, millimeter-wave (mmWave) communications, and massive multi-input and multi-output (MIMO) systems. To accommodate these technologies when investigating the cell search approach, in this paper, we consider a generic 5G cellular system, called multipath division multiple access (MDMA) system [30]–[32] in the literature.

As shown in Fig. 1, the MDMA system uses massive antenna technology in BSs and assumes a 30 GHz carrier frequency. In addition, it assumes that the distance between the BS antennas is several tens of wavelengths; the channel bandwidth is 200 MHz; and the radius of the cell is 50 m. Time division duplexing (TDD) is adopted in the system and the UL channel state information (CSI) is known at BS through channel estimation, which is used for DL precoding. The system assumes that the power control is executed in the uplink and that the universal frequency reuse is adopted. Thus, the MDMA system is interference limited. The MDMA system adopts the orthogonal frequency division modulation (OFDM) for transmission, and, for simplicity, we assume that the binary phase shift keying (BPSK) is used in this paper, though the extension to considering higher-order modulation is straightforward. In the system, rake receivers and pre-rake transmitters are used in the uplink and downlink respectively, where the rake receivers and pre-rake transmitters can be used to mitigate the multiple access interference (MAI) from other users in the same cell as well as the adjacent cell interference (ACI) from BSs and users in other cells.

Since the MDMA system considers using massive antenna technology which provides a large degree of freedom of spatial diversity, the multipath can be spatially resolved and the energy can be concentrated on a particular physical point of user via coherently combining the desired signals among received antennas. Such spatial focal point beamforming can thus let signal energy focus on the UE's geographical location, leading to significant performance improvement as compared to 4G cellular systems.

A. FRAME AND SYMBOL STRUCTURES

In the MDMA system, as shown in Fig. 2, a frame includes 25 blocks. Each time block consists of four slots including two uplink (UL) slots and two downlink (DL) slots. We assume that the duration of a slot is 10 μs, and thus the duration of a frame is 1ms. We assume the maximum velocity of vehicles is 108 km/hr, and the carrier frequency is 30 GHz. Hence, the coherence time is about 60 μs, implying that the channel impulse response is almost time-invariant among several time slots. Using this feature, the channel estimation for both DL and UL can be performed at the BS, leading to that the MDMA system is capable of performing the spatial focal point beamforming in both DL and UL. We assume that the DL slot can also be used to transmit the primary control tone (PCT) in frequency domain for the initial frequency synchronization. Note that to create the diversity for PCT, we would randomly select some antennas among all antennas for transmitting PCT. Such spatial-hopping mechanism during the transmission of PCT can thus help in dealing with hostile environments, e.g., environments with severe fading or interference.

Fig. 3 shows the symbol structure of the MDMA system. In the figure, we can see that there are both the DL and UL transmissions in a block, where the UL considers the data and pilot, and the DL considers the data and PCT. In addition, the PCT is located at the center of the frequency domain used for transmission. Note that since the energy of the PCT is focused on a single subcarrier, we generally assume the energy of the PCT subcarrier is much larger than the energy of other subcarriers.

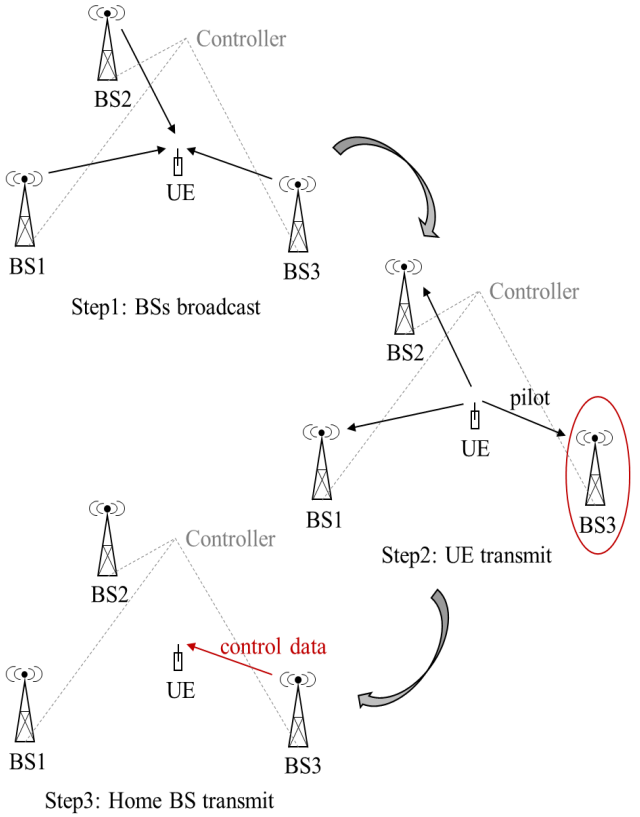

FIGURE 4. The schematic diagram of the proposed network resolved and mobile assisted cell search.

III. PROPOSED CELL SEARCH PROCEDURE

In traditional cell search methods, after completing the time and frequency synchronization, UE still needs to detect the cell ID based on the received control signal. For example, in WCDMA systems, after completing the time synchronization, UE still needs to perform scrambling code detection to identify the cell ID [6]. Similarly, in the LTE-A and typical 5G-NR systems, UE needs to perform SSS detection to identify the cell ID after the time and frequency synchronization [12], [20].

Different from the conventional methods, based on the generic MDMA system architecture, we in this paper propose a *Network Resolved and Mobile Assisted Cell Search.* As illustrated in Fig. 4, our proposed cell search considers that the BSs synchronized with one other are coordinated by the BS Controller (BSC). Then, the BSs controlled by the BSC regularly broadcast PCT to all UEs. A UE receiving the PCT would then use the PCT signal with cyclic prefix (CP) to complete the symbol time and frequency synchronization with all BSs. Then, the UE sends a universal uplink pilot code (p_0) to nearby BSs, and each BS calculates the power of the received pilot signal and sends the calculated value to the BSC. Based on these values, the BSC selects the BS with the highest received power as the home BS to serve the UE, which in Fig. 4 is BS3. Note that although the coordination of BSs in the considered network needs high-speed

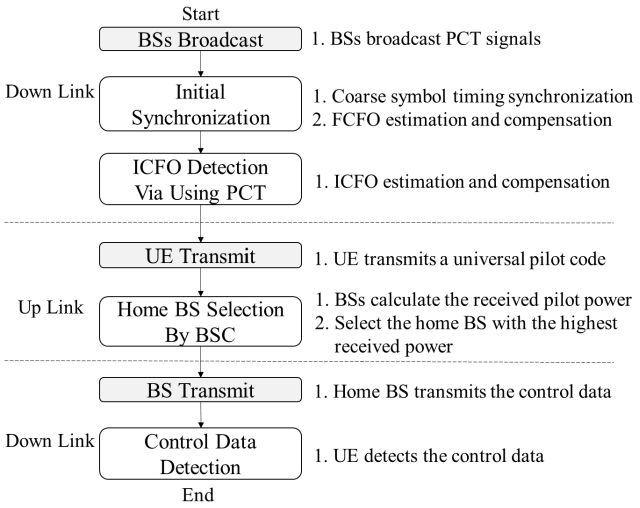

FIGURE 5. Initial cell search procedure.

connections between BSs for exchanging information, this is possible in the coordinated multi-point (CoMP) scenarios with cloud radio access networks (C-RANs) and/or remote radio heads (RRHs) [33].[1] In addition, since the CoMP scenario is envisioned for networks with small cells where large number of low-power devices, e.g., IoT devices, are expected to exist [34], such CoMP scenario consideration for realizing our proposed cell search approach indeed greatly matches our goal in this paper that the overhead of UEs should be offloaded to BSs.

After determining the home BS, the home BS estimates the channel using the pilot code (p_0) and transmits the related control data (such as frame header and user-specific pilot code, etc.) to the UE via focal point beamforming constructed by the Pre-RAKE precoding. Finally, the UE establishes a connection with the home BS by detecting the control data and starts the dedicated communications. It can be observed that by the above procedure, the UE does not need to detect the cell ID, while the BSs needs to conduct the received power computations and transmit the dedicated control data. Therefore, as compared to the conventional cell search approaches that requires the UE to detect the cell ID and decode the control data at beginning, a significant computation can be shifted to the BSs and/or the BSC, relieving the computational requirement for the UE. Based on the above principle, we will in the next section describe the proposed cell search approach in detail.

IV. PROPOSED CELL SEARCH APPROACH

In this section, we present the proposed cell search approach in detail. As illustrated in Fig. 5, the proposed cell search procedure consists of an initial synchronization, ICFO detection

[1] We note that in some scenarios, it is possible that some BSs are in sleep mode so that the network energy consumption can be reduced. When a BS is in sleep mode, the BS simply cannot receive the pilot signal transmitted by the UE, and thus does not participate in the coordination for initial cell search. However, when the BS is waken up, the BSC can coordinate the BS and let it join the coordination.

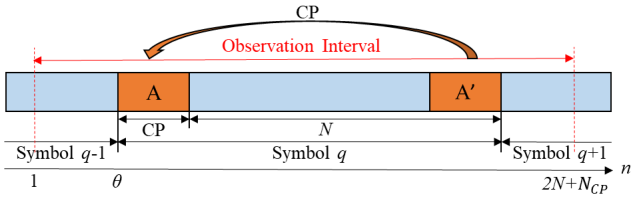

FIGURE 6. CP based auto-correlation.

via using PCT, and a home BS selection followed by a control data detection. To conduct the cell search for a UE, we assume the BSs can broadcast PCT signals for synchronization. In addition, we assume that the UE can transmit a pilot signal to BSs for home BS selection. Finally, we assume that the home BS can also transmit the control data to the UE. In the following, we will provide details of the main steps of the proposed cell search, respectively.

A. INITIAL SYNCHRONIZATION

We first provide the details of the initial synchronization. To conduct the synchronization, we use the characteristics of CP to estimate the symbol timing and the FCFO [32], [35]. Specifically, denoting that θ as the symbol timing offset and ε as the carrier frequency offset, the received signal of a UE can be expressed as:

$$r(n) = y(n-\theta)\exp(j2\pi\varepsilon n/N) + w(n), \tag{1}$$

where $y(n)$ is the received OFDM symbol without timing and carrier frequency offsets, n is the sample index of the OFDM symbol, N is the number of samples in a OFDM symbol, and w is the additive white Gaussian noise (AWGN). Then, as shown in Fig. 6, the CP is a replica of the transmitted signal at the tail of an OFDM symbol. Thus, we can estimate θ and ε by comparing the CP and the tail of the OFDM symbol. Based on this concept, we use the minimum mean-square error (MMSE) to estimate θ and ε:

$$\begin{aligned}
&(\hat{\theta},\hat{\varepsilon})\\
&= \arg\min_{\theta,\varepsilon}\left\{\sum_{n=\theta}^{\theta+N_{\mathrm{CP}}-1}\left|r(n)-r(n+N)e^{-j2\pi\varepsilon}\right|^2\right\}\\
&= \arg\min_{\theta,\varepsilon}\left\{\sum_{n=\theta}^{\theta+N_{\mathrm{CP}}-1}\begin{array}{l}(|r(n)|^2+|r(n+N)|^2\\ -r(n)r^*(n+N)e^{j2\pi\varepsilon}\\ -r^*(n)r(n+N)e^{-j2\pi\varepsilon})\end{array}\right\}\\
&= \arg\min_{\theta,\varepsilon}\left\{\begin{array}{l}\sum_{n=\theta}^{\theta+N_{\mathrm{CP}}-1}(|r(n)|^2+|r(n+N)|^2)\\ -2\mathrm{Re}\{\sum_{n=\theta}^{\theta+N_{\mathrm{CP}}-1}r(n)r^*(n+N)e^{j2\pi\varepsilon}\}\end{array}\right\}\\
&= \arg\max_{\theta,\varepsilon}\left\{\begin{array}{l}\left|\sum_{n=\theta}^{\theta+N_{\mathrm{CP}}-1}r(n)r^*(n+N)\right|\cos(\angle\gamma(\theta)+2\pi\varepsilon)\\ -\frac{1}{2}\sum_{n=\theta}^{\theta+N_{\mathrm{CP}}-1}(|r(n)|^2+|r(n+N)|^2)\end{array}\right\},
\end{aligned} \tag{2}$$

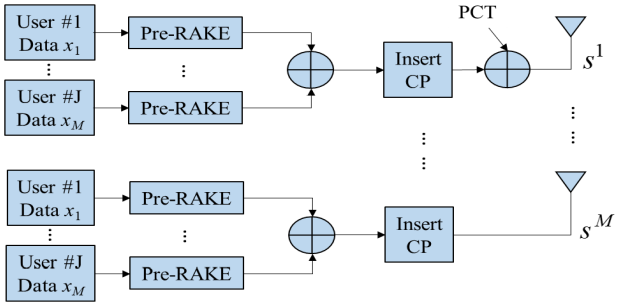

FIGURE 7. The block diagram of a DL transmitter (TX).

where N_{CP} is the number of samples of the CP and $\gamma(\theta) \equiv \sum_{n=\theta}^{\theta+N_{\mathrm{CP}}-1} r(n)r^*(n+N)$. By solving (2), we can obtain the following results:

$$\begin{aligned}
&\hat{\theta}_{\mathrm{MMSE}}\\
&= \arg\max_{\theta}\left\{\begin{array}{l}\left|\sum_{n=\theta}^{\theta+N_{\mathrm{CP}}-1}r(n)r^*(n+N)\right|\\ -\frac{1}{2}\sum_{n=\theta}^{\theta+N_{\mathrm{CP}}-1}\left[|r(n)|^2+|r(n+N)|^2\right]\end{array}\right\},
\end{aligned} \tag{3}$$

$$\hat{\varepsilon}_{\mathrm{MMSE}} = -\frac{1}{2\pi}\angle\gamma(\hat{\theta}_{\mathrm{MMSE}}), \tag{4}$$

where (3) is the estimated symbol timing offset that can be obtained by using exhaustive line search and (4) is the estimated FCFO.

B. ICFO DETECTION WITH PCT

After the initial synchronization, we use PCT to conduct estimate ICFO. As shown in Fig. 7, assuming without loss of generality that we use the first BS antenna to transmit the PCT signal, the transmitted signal of the antenna 1 of the BS ρ can be expressed as:

$$\begin{aligned}
s^{\rho,1}[n] = &\underbrace{\frac{1}{N}\sum_{k=0}^{N-1}\left(\sqrt{\frac{N}{2}}\delta[k-\frac{N}{2}]\right)e^{j2\pi kn/N}}_{\mathrm{PCT}}\\
&+\sum_{j=1}^{J}\underbrace{\sum_{l=0}^{L-1}\left(h_j^{\rho,1}[l]\right)^*\cdot x_j^{\rho}[n+l]}_{=\Theta_j^{\rho,1}},
\end{aligned} \tag{5}$$

where $s^{\rho,1}$ is the transmitted signal, $h_j^{\rho,1}[n]$ is the small-scale fading channel coefficient of path n between BS ρ and UE j, L is the number of paths, x_j is the UE j data, $\Theta_j^{\rho,m}$ is the UE j data after pre-RAKE precoding at antenna m, $N_{\mathrm{FFT}} = N$ is the length of the FFT/IFFT, and $\delta[.]$ is the Kronecker

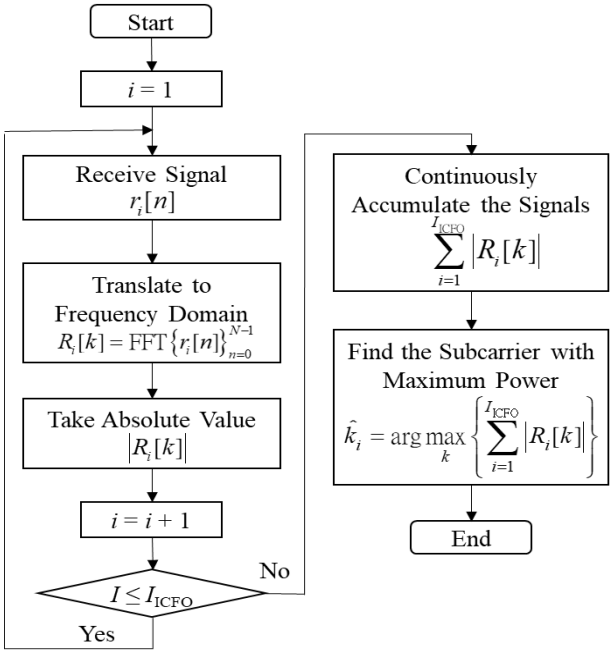

FIGURE 8. The flow chart of the ICFO Estimation.

delta. Similarly, the transmitted signal from BS ρ at antenna m without having PCT is expressed as:

$$s^{\rho,m}[n] = \sum_{j=1}^{J} \underbrace{\sum_{l=0}^{L-1} \left(h_j^{\rho,m}[l]\right)^* \cdot x_j^{\rho}[n+l]}_{=\Theta_j^{\rho,m}}. \tag{6}$$

Then, based on (5) and (6), the received signal by the UE j can be expressed as:

$$\begin{aligned} r_j^d[n] &= \sum_{\rho} (\beta^{\rho})^{1/2} \cdot \varsigma^{\rho} \sum_{m} s^{\rho,m}[n] * h_j^{\rho,m}[n] \\ &= \underbrace{\sum_{\rho} (\beta^{\rho})^{1/2} \cdot \varsigma^{\rho} \cdot \frac{1}{N} \sum_{k=0}^{N-1} \left(\sqrt{\frac{N}{2}} \delta[k - \frac{N}{2}] \right) e^{j2\pi kn/N} * h_j^{\rho,1}[n]}_{\text{PCT}} \\ &\quad + \underbrace{\sum_{\rho} \sum_{m} (\beta^{\rho})^{1/2} \cdot \varsigma^{\rho} \cdot \sum_{q=1}^{J} \Theta_q^{\rho,m}[n] * h_j^{\rho,m}[n] + w_j[n]}_{\text{User-Data}}, \end{aligned} \tag{7}$$

where β^{ρ} is the path loss factor, ζ^{ρ} is the shadow fading factor, and $*$ is the convolution operator. Following (7) and using the fundamental OFDM processing, we can obtain the OFDM symbol on subcarrier k as:

$$\begin{aligned} R_j^d[k] &= \mathrm{FFT}\left\{ r_j^d[n] \right\} \\ &= \underbrace{\sum_{\rho} \gamma^{\rho} \sqrt{\frac{N}{2}} \delta[k - \frac{N}{2} - \varepsilon_I] H_j^{\rho,1}[k - \varepsilon_I]}_{\text{PCT}} \\ &\quad + \underbrace{\sum_{\rho} \sum_{m} \gamma^{\rho} \mathrm{FFT}\left\{ \sum_{q=1}^{J} \Theta_q^{\rho,m}[n] \right\} H_j^{\rho,m}[k - \varepsilon_I]}_{\text{User-Data}} \\ &\quad + W_j[k - \varepsilon_I], \end{aligned} \tag{8}$$

where $\mathrm{FFT}\{.\}$ is the FFT operation, $\gamma^{\rho} = (\beta^{\rho})^{1/2} \cdot \varsigma^{c} \cdot e^{j2\pi k\theta/N}$, θ is the symbol time offset, and ε_I is the ICFO.

Finally, since we assume a TDD system, the UE would receive both the DL signals from the BSs and UL signals from other UEs. Specifically, the received signal of the UE in the UL slot is the combination of UL signals from other UEs. Thus, when in UL slot, the received signal can be written as:

$$r_j^u[n] = \sum_{\rho} \sum_{q=1}^{J} (\beta_{q,j}^{\rho})^{1/2} \cdot \varsigma_{q,j}^{\rho} \cdot x_q^{\rho}[n] * h_{q,j}^{\rho}[n], \tag{9}$$

where $h_{q,j}^{\rho}[n]$ is the small-scale fading channel coefficient of path n between UE j and UE q in cell ρ.

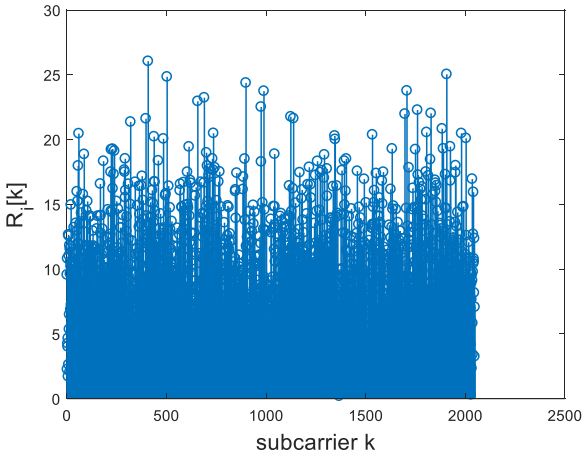

FIGURE 9. The example of the frequency domain before the energy combing, where $i = 1$.

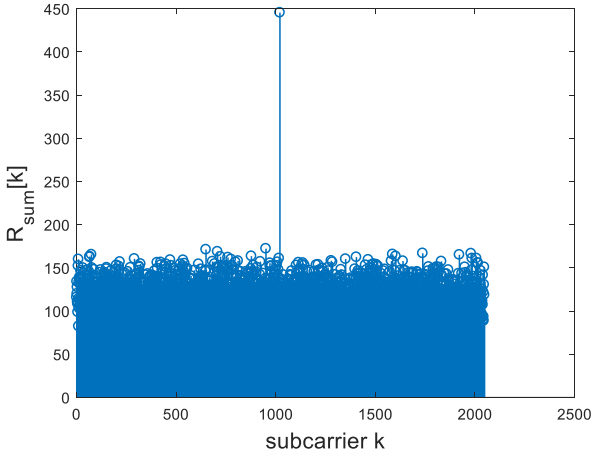

FIGURE 10. The example of the frequency domain after the energy combing.

TABLE 1. Collision probability.

N_{BS} \ N_{UE}	1	2	4
100	1.15×10^{-6}	2.3×10^{-6}	4.6×10^{-6}
1000	1.15×10^{-5}	2.3×10^{-5}	4.6×10^{-5}
10000	1.15×10^{-4}	2.3×10^{-4}	4.6×10^{-4}

Fig. 8 is the overall flow chart of the PCT detection. Specifically, the UE j continuously receives I_{ICFO} symbols and then converts the received symbols to the frequency domain as:

$$R_i[k] = \text{FFT}\left\{r_i[n]\right\}_{n=0}^{N-1}, \tag{10}$$

where $r_i[n]$ is sample n of the received symbol i of UE j. Then, we find the subcarrier $\hat{k}_i$ with the maximum power after the energy combining of received symbols, given as:

$$\hat{k}_i = \arg\max_{k} \left\{ \sum_{i=1}^{I_{\text{ICFO}}} |R_i[k]| \right\}. \tag{11}$$

Due to that the interference and noise are random, the interference and noise could be suppressed after the combining, and thus the subcarrier with the maximum power is considered as the subcarrier with PCT, which is then used for ICFO detection.

Figs. 9 and 10 show an example of the frequency domain before and after the energy combining. We can see that the PCT can be highlighted, and the interference and noise can be effectively suppressed by the combining.

C. HOME BS SELECTION

The previous two steps are for time and frequency synchronization in the cell search. After finishing the synchronization, the UE would transmit a pilot signal back to the BSs. Then, the BSs receiving the pilot signal can cooperatively decide which BS would serve as the home BS to serve the UE. The details of the home BS selection are provided in the following.

Specifically, we assume that the UE after time and frequency synchronization sends a universal pilot code p_0 to all BSs. Note that since the initial cell search only happens when the UE boots up or when the UE completely lost the signal of the network, the probability of two UEs to conduct the initial cell search at the same time is very low. Therefore, all UEs might use the same pilot code. The collision probability assuming that all UEs use the same pilot code is shown in Table 1, where N_{UE} is the number of times for each UE to boot up in a day, and N_{BS} is the number of UEs for each BS to serve in a day. The analysis for the collision probability is detailed in the appendix A. Note that if we would like to further reduce the collision probability, the simple code-division multiple access approach can be conducted.

After the BSs receive the pilot signal, BSs calculate the power of the received pilot signal and send the results to the BSC. The BSC then selects the BS with the maximum power as the Home BS. To conduct the power calculation, assuming that UE j sends the universal pilot code p_0 to the nearby BSs, the received signal for antenna m at BS ρ can be expressed as:

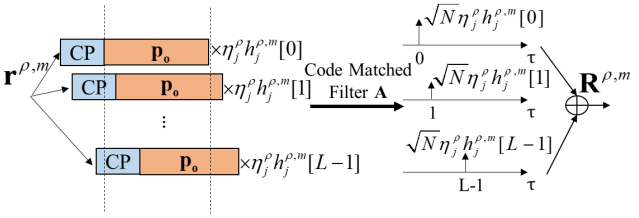

FIGURE 11. The channel estimation based on code match filter.

$$\begin{aligned} r^{\rho,m}[n] = {} & \alpha_j \cdot \underbrace{(\beta_j^\rho)^{1/2} \cdot \varsigma_j^\rho \cdot p_0[n] * h_j^{\rho,m}[n]}_{\text{pilot}} \\ & + \underbrace{\sum_{\substack{q=1 \\ q\neq j}}^{J} \alpha_q \cdot (\beta_q^\rho)^{1/2} \cdot \varsigma_q^\rho \cdot x_q^\rho[n] * h_q^{\rho,m}[n]}_{\text{MAI}^{\text{m}}} \\ & + \text{OCI}^m + w^{\rho,m}[n], \end{aligned} \tag{12}$$

where α_j is the power control factor determined by the UE according to the power of the PCT received by the UE j; MAI^m is the interference of other UEs in the same cell at antenna m; and OCI^m is the interference of other cells at antenna m. Note that the MAI and OCI exist even though UE j is the only UE that is conducting the cell search, as its pilot signal might still be interfered by UEs sending common control and/or data signal. Based on (12), in following, we discuss how the UE can determine the power control factor and how the BSs can calculate the power of the received pilot signal.

1) POWER CONTROL FACTOR DETERMINATION

Assume that UE j continuously receives I_{P} downlink signals and calculates the average power of the PCT. Suppose we want to let the average UL pilot power received at the BSs to be approximately Q times of the standard received signal power P_{Ref} predefined by the system configuration. Then, in this case, the transmit power of the UE needs to be $P_j = \alpha_j P_{\text{Ref}}$, where α_j can be calculated by:

$$\alpha_j = \frac{QP_{\text{PCT}}}{\frac{1}{I_{\text{P}}}\sum_{i=1}^{I_{\text{P}}} \left| R_{j,i}^d[\frac{N}{2} + \varepsilon_{\text{I}}] \right|^2}, \tag{13}$$

where P_{PCT} is the average transmit power of PCT predetermined according to the system configuration and $R_{j,i}^d$ has been defined in equation (8).

2) RECEIVED PILOT POWER CALCULATION

Here, we discuss how to calculate the received pilot power. Specifically, we first reformulate (12) as:

$$\begin{aligned} & r^{\rho,m}[n] \\ & \quad = \eta_j^\rho \cdot p_0[n] * h_j^{\rho,m}[n] + \text{Interference} \end{aligned}$$

$$= \eta_j^{\rho} \cdot \sum_{l=0}^{L-1} h_j^{\rho,m}[l] \cdot p_0[(n-l) \bmod N] + \text{Interference}, \tag{14}$$

where $\eta_j^{\rho} = \alpha_j \cdot (\beta_j^{\rho})^{1/2} \cdot \varsigma_j^{\rho}$; and *Interference* includes MAI^m, OCI^m and $w^{\rho,m}$. Then, the vectorization of $r^{\rho,m}[n]$ can be expressed as:

$$\begin{aligned} \mathbf{r}^{\rho,m} &= [r^{\rho,m}[0] r^{\rho,m}[1] \cdots r^{\rho,m}[N-1]] \\ &= \eta_j^{\rho} \sum_{l=0}^{L-1} h_j^{\rho,m}[l] \cdot \mathbf{p}_0^{(l)} + \mathbf{I}, \end{aligned} \tag{15}$$

where $\mathbf{I}$ is the corresponding vectorization of the interference and $\mathbf{p}_0^{(l)}$ is the l-tap cyclic shift of the vector $\mathbf{p}_0$. Note that the exact mathematical expression is given as follows:

$$\mathbf{p}_0^{(l)} \triangleq [p_0[l] \cdots p_0[N-1] \quad p_0[0] \cdots p_0[l-1]]. \tag{16}$$

Next, as illustrated in Fig. 11, we use the pilot code $\mathbf{p}_0$ to match $r^{\rho,m}[n]$. This thus give rise to:

$$\mathbf{R}^{\rho,m} = \mathbf{A} \cdot \mathbf{r}^{\rho,m} = [R^{\rho,m}[0] R^{\rho,m}[1] \cdots R^{\rho,m}[L-1]], \tag{17}$$

where $\mathbf{A}$ is the cyclic impulse response of $\mathbf{p}_0$ given as:

$$\mathbf{A} \equiv \frac{1}{N} \begin{bmatrix} p_0^*[0] & p_0^*[1] & \cdots & p_0^*[N-1] \\ p_0^*[N-1] & p_0^*[0] & \cdots & p_0^*[N-2] \\ \vdots & \vdots & \ddots & \vdots \\ p_0^*[N-L+1] & p_0^*[N-L+2] & \cdots & p_0^*[N-L] \end{bmatrix}. \tag{18}$$

We then perform the path selection that selects N_p paths from $\mathbf{R}^{\rho,m}$. This thus gives:

$$\begin{aligned} \hat{\mathbf{R}}^{\rho,m} &= f(\mathbf{R}^{\rho,m}) = [R^{\rho,m}[\tau_1] R^{\rho,m}[\tau_2] \cdots R^{\rho,m}[\tau_{N_p}]], \\ &\tau_k \in \{0, 1, \ldots, L-1\}, \end{aligned} \tag{19}$$

where τ_k is the delay of selected k path index, $f(\cdot)$ represents the path selection process as in [36]. After normalizing $\hat{\mathbf{R}}^{\rho,m}$, we then obtain the estimated channel:

$$\hat{\mathbf{h}}_j^{\rho,m} = \frac{\hat{\mathbf{R}}^{\rho,m}}{\| \hat{\mathbf{R}}^{\rho,m} \|}. \tag{20}$$

Given (20), we then conduct equalization and coherently combining for the received pilot signal at all antennas. This thus leads to:

$$\begin{aligned} r^{\rho}[n] &= \sum_{m=1}^{M} r^{\rho,m}[n] * (\hat{h}_j^{\rho,m}[L-1-n])^* \\ &= \sum_{m=1}^{M} \alpha_j \cdot (\beta_j^{\rho})^{1/2} \cdot \varsigma_j^{\rho} \cdot p_0[n] * h_j^{\rho,m}[n] \\ &\quad * (\hat{h}_j^{\rho,m}[L-1-n])^* + \text{MAI} + \text{OCI} + \text{W} \\ &\cong \alpha_j \cdot (\beta_j^{\rho})^{1/2} \cdot \varsigma_j^{\rho} \cdot M \cdot p_0[n] + \text{ISI} + \text{MAI} \\ &\quad + \text{OCI} + \text{W}. \end{aligned} \tag{21}$$

TABLE 2. Simulation parameters.

Parameter	Value
Carrier frequency, f_c	30 GHz
Total transmission bandwidth, B_W	200 MHz
Bit time, T_c	5 ns
Maximum delay spread, τ_{max}	400 ns
Number of antennas at BS, M	300
Radius of cellular, R	50 m
Number of users in one cell, J	10,20,...,100
The maximum velocity of MS, v_{max}	108 km/hr
Length of slot, N_{slot}	2208 tap
FTT size, N	2048 tap
Length of ZC sequence, N_{ZC}	2053 tap
User energy in one slot, E_u	1 unit
PCT energy in one slot, E_{PCT}	0.5 unit

Then, based on this, the BSC can select the Home BS according to the power, given as:

$$\hat{\rho} = \arg\max_{\rho} \left\{ \frac{1}{N} \sum_{n=1}^{N} \left| r^{\rho}[n] \right|^2 \right\}. \tag{22}$$

Based on (22), we can extend the home BS selection to accommodating more observations, as we make the selection after collecting results from multiple symbols. Specifically, suppose that the observation is across I_{Sel} symbols. The Home BS selection result can be given by

$$\hat{\rho} = \arg\max_{\rho} \left\{ \frac{1}{N I_{Sel}} \sum_{i=1}^{I_{Sel}} \sum_{n=1}^{N} \left| r_i^{\rho}[n] \right|^2 \right\}. \tag{23}$$

D. CONTROL DATA DETECTION

After the home BS is determined, we can proceed to the control data detection. Specifically, after the BSC determines the home BS, it transmits the pre-RAKE control data to UE j. Since the control data is dedicatedly for the UE, there is no need to broadcast the control data to all UEs like the traditional cell search methods. As a result, all complicated calculations for the control data can be performed on the home BS. The UE only needs to detect the pre-RAKE control data to establish the connection with the home BS, and thus as compared to the conventional cell search approaches that requires the UE to detect the cell ID and decode the control data, e.g., decode the frame header and find the user-specific pilot code, at beginning, a significant computation can be shifted to the BSs and/or the BSC.

To this end, the proposed initial cell search has been discussed in detail. In the next section, we will perform simulations to evaluate the proposed cell search approach.

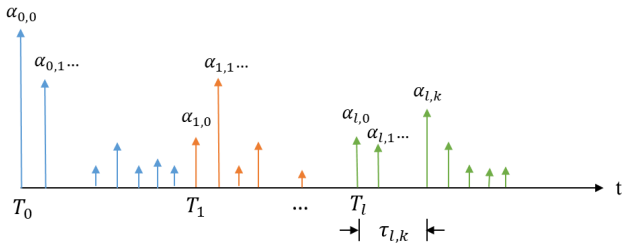

FIGURE 12. Typical channel realization of the S-V model.

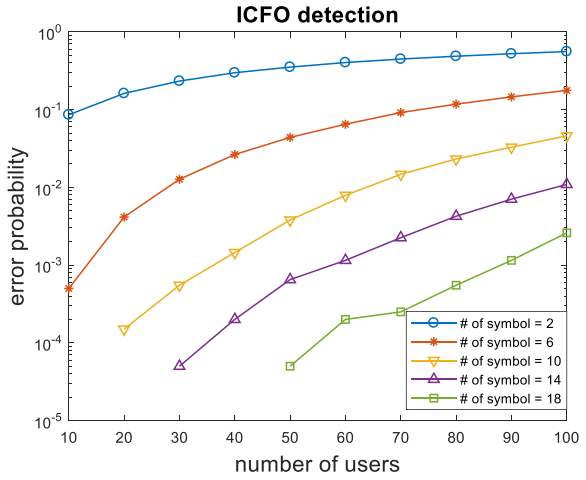

FIGURE 13. The error probability of ICFO detection.

V. NUMERICAL RESULTS AND COMPARISONS

In this section, we use simulations to evaluate the proposed initial cell search approach.

A. SIMULATION SETUP

In simulations, we consider the interference-limited MDMA cellular system with the basic architecture as described in [30] and the basic parameters as provided in Table 2, where the noise effect is ignored for simplicity. Specifically, we consider the carrier frequency $f_c = 30$ GHz with bandwidth$B_W = 200$ MHz. Hence, the bit time is given as $T_c = 1/B_W = 5$ ns. We assume the maximum delay spread to be $\tau_{\max} = 400$ ns and set the number of antennas at BS as $M = 300$. Because the pathloss attenuation of mmWave communication is severe, we consider the small cell BSs to serve the area with radius $R = 50$ m. We set the length of a complete OFDM symbol as $N_{\text{slot}} = 2208$ tapand the length of CP as $N_{\text{CP}} = 160$ tap. We let the FFT size be $N = 2048$ and use a ZC-sequence for the universal pilot. Since we consider interference-limited system, the exact unit of the transmit power is not critical. We thus set the UE data energy in one slot be 1 unit and the PCT energy in one slot is 0.5 unit without otherwise indicated.

A mmWave S-V channel model combining results in [37] and [38] is adopted for simulations. As illustrated in Fig. 12, the channel impulse response is divided into multiple clusters, and each cluster contains many rays. As long as the bandwidth is wide enough, these paths can be clearly distinguished, leading to that the equivalent baseband impulse

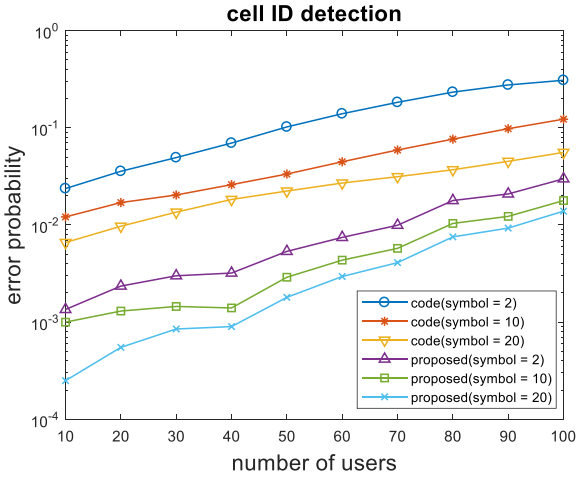

FIGURE 14. Comparisons between the proposed cell search and the code-based cell search approaches in terms of the cell ID detection error probability under different observation symbols.

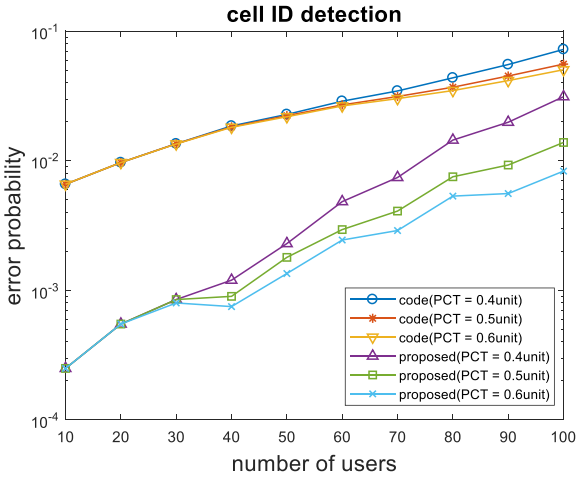

FIGURE 15. Comparisons between the proposed cell search and the code-based cell search approaches in terms of the cell ID detection error probability under different PCT energies.

response is expressed as:

$$\tilde{h}(t) = \sum_{l=0}^{\infty}\sum_{k=0}^{\infty} \alpha_{l,t} e^{j\phi_{l,k}} \delta(t - T_l - \tau_{l,k}), \tag{24}$$

where l, k, α, ϕ, T, and τ are respectively the cluster index, ray index, path amplitude gain, phase shift, cluster arrival time, and ray arrival time. We assume that both the clusters and the rays follow the Poisson process and assume that both the cluster power and power of ray path in each cluster decays exponentially with respect to time.

B. SIMULATION RESULT

In this subsection, we evaluate the proposed initial cell search approach. We first evaluate the error rate of the ICFO estimation in Fig. 13 as a function of the number of users simultaneously served by the BS, where the error probability of ICFO detection refers to as the probability that the PCT is incorrectly detected, and different numbers of symbols of different curves refer to as using different numbers of symbols

TABLE 3. Analytical computational complexity.

	Code-based	Proposed network resolved
Initial synchronization	Same (at UE side)	Same (at UE side)
ICFO detection	Same (at UE side)	Same (at UE side)
Home BS selection	$(3\times\frac{N}{2}\log_2 N+2N)\times N_{Code}$ (at UE side)	$(3\times\frac{N}{2}\log_2 N+2N)\times N_T\times N_{Cell}$ (at BS side)

to conduct the combining in (11) when detecting the PCT. Results show that our ICFO detection is effective and the accuracy can be better than 10^{-2} when the number of symbols is as small as 14. Also, results show that when increasing the number of symbols for combining, the error probability can be decreased as expected.

Figs. 14 and 15 evaluate the cell search error probability, where the error probability refers to as the probability that the BS with the largest received power is not selected by the corresponding cell search approach. Note that here we assume the cell search would fail if the initial synchronization and ICFO detection fail. In addition, we compare our proposed cell search method with the conventional code-based cell search method. The reason for adopting the code-based cell search method as the reference scheme for comparison is that the conventional 3G, 4G and 5G mobile networks all use different codes to identify different BSs. Hence, it is representative to compare our proposed method with such code-based method. Note that for the code-based method in simulations, the ZC-sequences are used as the cell identification codes. We assume that the initial synchronization and the ICFO detection provided in this paper are adopted by both our proposed cell search and the reference code-based method for fair comparison.

Fig. 14 compares between the proposed cell search and the code-based cell search with different numbers of observation symbols I_{Sel}. We see that the proposed cell search method can always outperform the corresponding code-based method when they have the same number of observation symbols. Furthermore, we can see that even if the proposed cell search has a smaller number of observation symbols than that of the coded-based cell search, the proposed cell search can still be better.

Finally, considering that the number of observation symbols is 20, Fig. 15 compares between the proposed cell search and the code-based cell search considering different PCT energies. Results again show that the proposed approach can outperform the code-based cell search, validating the efficacy of the proposed approach.

C. COMPUTATIONAL COMPLEXITY AND ENERGY CONSUMPTION ANALYSIS

In this subsection, we discuss the computational complexity and energy consumption of the network for conducting the initial cell search of a UE. Specifically, we first calculate the computational complexity of the proposed cell search and the representative code-based cell search. Then, based on the computational complexity results, we calculate the computational energy consumption of the network. Finally, we discuss the transmit power consumption of the initial cell search approaches.

We first calculate the computational complexity of the proposed cell search and the code-based cell search. Note that since the numbers of complex additions and complex multiplications are orderwise similar and a complex multiplication is much more costly than a complex addition, we herein focus on the analysis in terms of complex multiplications. The complexity of each step of two cell search methods is provided in Table 3, where N_{Code} is the number of codes that indicate the cell IDs in code-based cell search; N_{T} is the number of BS antennas for one sector; and N_{Cell} is the number of the BSs for a UE to select in the proposed network resolved cell search. Basically, the initial synchronization and ICFO detection conducted on the UE side are the same for both the code-based and proposed cell search approaches. Thus, the difference lies in that the home BS selection for the code-based cell search is on UE side, while the home BS selection for the proposed cell search is on BS side. For code-based cell search, the detection of home BS requires to check every possible code and each code requires three FFT operations along with additional $2N$ complex multiplications to decode. Since each FFT operation requires $N\log_2(N)/2$ complex multiplications, the detection of N_{Code} codes in total requires $N_{\text{Code}}(3N\log_2(N)/2+2N)$ complex multiplications. On the other hand, the proposed network resolved cell search requires each antenna of BS to conduct three FFT operations with $2N$ complex multiplications to decode the pilot signal transmitted by the UE. Therefore, since we consider that N_{Cell} BSs participate in the home BS selection and each BS has N_{T} antennas, we in total require $N_{\text{T}}N_{\text{Cell}}(3N\log_2(N)/2+2N)$ complex multiplications for the proposed cell search approach.

To numerically compare the complexity, we consider $N=2048$, $N_{\text{Code}}=504$, $N_{\text{T}}=100$, and $N_{\text{Cell}}=7$. Therefore, according to Table 3 we observe that the number of complex multiplications for the home BS selection of code-based cell search is 19.1×10^6; for the home BS selection of the proposed cell search is 26.5×10^6. We see that although the proposed cell search has slightly larger complexity, their difference is not large. Furthermore, since the home BS selection of the proposed cell search is on the BS side, it offloads the computational cost from the UEs to BSs. To evaluate such offloading in terms of the energy consumption saved by the UE, using Table 1 of [39], we can consider that the energy consumption to perform a single complex multiplication is 1.5×10^{-3} nJ in the circuit made by the 28 nm technology. It follows that the energy consumptions to complete the cell search of a UE are 29 μJ and 40 μJ for the code-based and proposed network resolved cell search approaches, respectively. The results indicate that the overall computational energy consumptions for both cell search approaches are similar.

We now compare the transmit power consumptions of both cell search approaches. Note that since the exact transmit power consumption depends on the specific details of the adopted transmission strategy and protocol, we in the following conduct the comparison based only on the rough picture of two cell search approaches. Since both cell search approaches require the same initial synchronization and ICFO detection, the power consumption due to them is the same. We thus focus on the power consumption for the home BS selection. It follows that for the code-based cell search, the UE needs to first transmit a registration signal to tell BSs that the synchronization and selection has been completed, and then the BSs transmit the control signal to the connected UE. On the other hand, for the proposed network resolved cell search, the UE needs to first transmit the universal pilot signal to BSs for home BS selection, and then the home BS transmits an ACK to UE indicating that the home BS selection is complete with the control signal. Therefore, the transmit power consumptions for both cell search approaches are generally the same.

By the above discussions, we see that overall energy consumptions for conducting the code-based cell search and the proposed network resolved cell search approaches are similar. Then, since our proposed approach can offload the computational cost to the BSs, it is advantageous when the UEs have limited computational capability and require low energy consumption.

VI. CONCLUSION

In this paper, we proposed a novel *Network Resolved and Mobile Assisted Cell Search* method that can improve the experience of UE by offloading the computational overhead of cell search to BSs. This thus can reduce the battery consumption of the UE and improve the UE experiences as all the complicated calculations can be completed by the BSs, instead of the UEs. The detailed procedure of the proposed cell search method was presented. Simulations results showed that in addition to the benefit of computational offloading of the UEs, the proposed cell search method can outperform the conventional code-based cell search method in terms of the cell search error probability.

APPENDIX

THE COLLISION PROBABILITY

We use the Erlang B model to calculate the collision probability:

$$B = \frac{A^N}{N! \sum_{i=0}^{N} \frac{A^i}{i!}}. \tag{25}$$

We assume that the number of service channels is $N = 1$ and that the traffic volume $A = \lambda H$, where $\lambda = (N_{\mathrm{UE}} \times N_{\mathrm{BS}})/(24 \times 3600)$ is the arrival rate with each N_{UE} being the number of boot-up for a UE in a day and N_{BS} being number of UEs served by a BS; and $H = 1$ ms is the service frame time. By plugging the above parameters into (25), the blocking rate can be obtained as follows:

$$B = \frac{A}{1+A} \cong H \times (N_{UE} \times N_{BS})/(24 \times 3600). \tag{26}$$

REFERENCES

[1] G. Lui and H. Tan, "On joint symbol and frame synchronization for direct-detection optical communication systems," *IEEE Trans. Commun.*, vol. COM-35, no. 2, pp. 250–255, Feb. 1987.

[2] M. Li and W. Zhang, "A novel method of carrier frequency offset estimation for OFDM systems," *IEEE Trans. Consum. Electron.*, vol. 49, no. 4, pp. 965–972, Nov. 2003.

[3] S. Won and S. W. Choi, "A tutorial on 3GPP initial cell search: Exploring a potential for intelligence based cell search," *IEEE Access*, vol. 9, pp. 100223–100263, 2021.

[4] T. S. Rappaport, *Wireless Communications: Principles and Practice*, 2nd ed., Upper Saddle River, NJ, USA: Prentice-Hall, 2002.

[5] A. Mehrotra, *GSM System Engineering*. Boston, MA, USA: Artech House, 1997.

[6] *Universal Mobile Telecommunications System (UMTS); Spreading and Modulation (FDD)*, 3GPP, Standard TS 25.213 v3.4.0, 2000.

[7] *Physical Channels and Mapping of Transport Channels Onto Physical Channels (FDD)*, 3GPP, Standard TS 25.211 v12.0.0, 2014.

[8] S. K. Bahl, "Cell searching in WCDMA," *IEEE Potentials*, vol. 22, no. 2, pp. 16–19, Apr. 2003.

[9] Y. P. E. Wang and T. Ottosson, "Cell search in W-CDMA," *IEEE J. Sel. Areas Commun.*, vol. 18, no. 8, pp. 1470–1482, Aug. 2000.

[10] T. Imai and S. Mori, "Analysis of cell search performance for W-CDMA cellular system," *Electron. Commun. Jpn., I, Commun.*, vol. 88, no. 5, pp. 67–78, May 2005.

[11] M. K. Song and V. K. Bhargava, "Performance analysis of cell search in W-CDMA systems over Rayleigh fading channels," *IEEE Trans. Veh. Technol.*, vol. 51, no. 4, pp. 749–759, Jul. 2002.

[12] *Physical Channels and Modulation*, 3GPP, Standard TS 36.211 v12.6.0, 2015.

[13] S. Sesia, I. Toufik, and M. Baker, *LTE—The UMTS Long Term Evolution, From Theory to Practice*. Hoboken, NJ, USA: Wiley, 2011.

[14] E. Dahkman, S. Parkvall, and J. Skold, *4G: LTE/LTE-Advanced for Mobile Broadband*, 2nd ed. Cambridge, MA, USA: Academic, 2013.

[15] *1MA150: Cell Search and Cell Selection in UMTS LTE*, Rohde & Schwarz, Munich, Germany, 2009, pp. 1–40.

[16] P.-Y. Tsai and H.-W. Chang, "A new cell search scheme in 3GPP long term evolution downlink, OFDMA systems," in *Proc. Int. Conf. Wireless Commun. Signal Process.*, Nanjing, China, Nov. 2009, pp. 1–5.

[17] K. Manolakis, D. M. Gutierrez Estevez, V. Jungnickel, W. Xu, and C. Drewes, "A closed concept for synchronization and cell search in 3GPP LTE systems," in *Proc. IEEE Wireless Commun. Netw. Conf.*, Apr. 2009, pp. 1–6.

[18] *Making 5G NR a Reality, Qualcomm Research Document*, Qualcomm Incorporated, San Diego, CA, USA, Dec. 2016, pp. 1–26.

[19] *Study on New Radio (NR) Access Technology; Physical Layer Aspects*, 3GPP, Standard TR 38.802 v2.0.0, 2017.

[20] *NR; Physical Layer; General Description*, 3GPP, Standard TS 38.201 v15.0.0, 2017.

[21] *NR; Physical Channels and Modulation*, 3GPP, Standard TS 38.211 v15.5.0, 2019.

[22] *NR; Physical Layer Procedures for Control*, 3GPP, Standard TS 38.213 v15.5.0, 2019.

[23] *Study on New Radio (NR) Access Technology*, 3GPP, Standard TR 38.912 v16.0.0, 2020.

[24] D. Wang, Z. Mei, H. Zhang, and H. Li, "A novel PSS timing synchronization algorithm for cell search in 5G NR system," *IEEE Access*, vol. 9, pp. 5870–5880, 2021.

[25] M. Wang, D. Hu, L. He, and J. Wu, "Deep-learning-based initial access method for millimeter-wave MIMO systems," *IEEE Wireless Commun. Lett.*, vol. 11, no. 5, pp. 1067–1071, May 2022.

[26] D. Inoue, K. Ota, M. Sawahashi, and S. Nagata, "Physical cell ID detection using joint estimation of frequency offset and SSS sequence for NR initial access," *IEICE Trans. Commun.*, vol. E104.B, no. 9, pp. 1120–1128, 2021.

[27] *5G Non-Public Networks for Industrial Scenarios*, 5G Alliance for Connected Industries and Automation (5GACIA), Frankfurt am Main, Germany, July 2019, pp. 5–14.

[28] B. Chen, J. Wan, L. Shu, P. Li, M. Mukherjee, and B. Yin, "Smart factory of industry 4.0: Key technologies, application case, and challenges," *IEEE Access*, vol. 6, pp. 6505–6519, 2017.
[29] J. G. Andrews, S. Buzzi, W. Choi, S. V. Hanly, A. Lozano, A. C. K. Soong, and J. C. Zhang, "What will 5G be?" *IEEE J. Sel. Areas Commun.*, vol. 32, no. 6, pp. 1065–1082, Jun. 2014.
[30] W. H. Hsiao and C. C. Huang, "A novel 5G TDD cellular system proposal based on multipath division multiple access," in *Proc. 19th Int. Conf. Adv. Commun. Technol. (ICACT)*, Feb. 2017, pp. 936–942.
[31] W. H. Hsiao and C. C. Huang, "A study on the fifth generation mobile communication system based on multipath division multiple access," Ph.D. dissertation, Dept. Electron. Inf. Eng., Nat. Chiao Tung Univ., Hsinchu, Taiwan, 2018.
[32] K.-L. Chiu, P.-H. Shen, B.-R. Lin, W.-H. Hsiao, S.-J.-J. Jou, and C.-C. Huang, "Design of downlink synchronization for millimeter wave cellular system based on multipath division multiple access," *IEEE Trans. Circuits Syst. I, Reg. Papers*, vol. 67, no. 9, pp. 3211–3223, Sep. 2020.
[33] *Coordinated Multi-Point Operation for LTE Physical Layer Aspects*, 3GPP, Standard TR 36.819 v11.0.0, 2011.
[34] V. Jungnickel, K. Manolakis, W. Zirwas, B. Panzner, V. Braun, M. Lossow, M. Sternad, R. Apelfröjd, and T. Svensson, "The role of small cells, coordinated multipoint, and massive MIMO in 5G," *IEEE Commun. Mag.*, vol. 52, no. 5, pp. 44–51, May 2014.
[35] D. Lee and K. Cheun, "Coarse symbol synchronization algorithms for OFDM systems in multipath channels," *IEEE Commun. Lett.*, vol. 6, no. 10, pp. 446–448, Oct. 2002.
[36] M.-L. Ku and C.-C. Huang, "A complementary codes pilot-based transmitter diversity technique for OFDM systems," *IEEE Trans. Wireless Commun.*, vol. 5, no. 3, pp. 504–508, Mar. 2006.
[37] M. R. Akdeniz, Y. Liu, M. K. Samimi, S. Sun, S. Rangan, T. S. Rappaport, and E. Erkip, "Millimeter wave channel modeling and cellular capacity evaluation," *IEEE J. Sel. Areas Commun.*, vol. 32, no. 6, pp. 1164–1179, Jun. 2014.
[38] A. A. M. Saleh and R. A. Valenzuela, "A statistical model for indoor multipath propagation," *IEEE J. Sel. Areas Commun.*, vol. SAC-5, no. 2, pp. 128–137, Feb. 1987.
[39] D. Esposito, D. De Caro, E. Napoli, N. Petra, and A. G. M. Strollo, "On the use of approximate adders in carry-save multiplier-accumulators," in *Proc. IEEE Int. Symp. Circuits Syst. (ISCAS)*, May 2017, pp. 1–4.

JIA-LE YIN received the B.S. degree from the Department of Information and Electronic Engineering, Zhejiang University (ZJU). He is currently pursuing the Ph.D. degree with the Institute of Communications Engineering, National Yang-Ming Chiao-Tung University (NYCU). His research interest includes cell search for next-generation mobile communication systems.

MING-CHUN LEE (Member, IEEE) received the B.S. and M.S. degrees in electrical and computer engineering from the National Chiao Tung University, Hsinchu, Taiwan, in 2012 and 2014, respectively, and the Ph.D. degree from the Ming Hsieh Department of Electrical Engineering, University of Southern California, in 2020. From 2014 to 2016, he was a Research Assistant with the Wireless Communications Laboratory, Research Center for Information Technology Innovation, Academia Sinica, Taiwan. He is currently an Assistant Professor with the Institute of Communications Engineering, National Yang Ming Chiao Tung University. His research interests include signal processing, and design, modeling, and analysis in wireless systems and networks. He is especially working on topics relevant to caching, computing, and communication in wireless networks and integrated sensing and communication systems in recent years. He received the USC Annenberg Fellowship from 2016 to 2020. He was awarded the Exemplary Reviewer of the IEEE TRANSACTIONS ON COMMUNICATIONS in 2019.

WEI-HAN HSIAO (Member, IEEE) received the B.S. degree in electrical and control engineering and the Ph.D. degree in communications engineering from the National Yang Ming Chiao Tung University (NYCU), Taiwan, in 2008 and 2018, respectively. From 2018 to 2021, he worked as a Senior Engineer at the Foxconn Advanced Communication Academy, HonHai (Foxconn), engaging in 5G NR Cloud RAN and O-RAN Project. Since September 2021, he has been with the Department of Electrical Engineering, Chang Gung University, Taiwan. He is currently an Assistant Professor. His research interests include next generation 5G/B5G/6G mobile communication systems, millimeter wave massive MIMO technologies, and cellular communication systems.

CHIA-CHI HUANG was born in Taiwan. He received the B.S. degree in electrical engineering from the National Taiwan University, in 1977, and the M.S. and Ph.D. degrees in electrical engineering from the University of California at Berkeley, Berkeley, CA, USA, in 1980 and 1984, respectively.

From 1984 to 1988, he was an RF and Communication System Engineer with the Corporate Research and Development Center, General Electric Company, Schenectady, NY, USA, where he worked on mobile radio communication system design. From 1989 to 1992, he was with the IBM T. J. Watson Research Center, Yorktown Heights, NY, USA, as a Research Staff Member, working on indoor radio communication system design. Since 1992, he has been with the National Yang Ming Chiao Tung University, Hsinchu, Taiwan, and he was a Professor with the Department of Electrical and Computer Engineering until his retirement, in February 2021. His research interests include mobile radio, wireless communications, and cellular systems.